Singularity-Free Path Following Control for Miniature Unmanned Helicopters

Xujie Ma and Wei Huo

Abstract A singularity-free nonlinear controller is presented for the miniature unmanned helicopter to follow a reference path described by implicit expressions. Based on the time-scale separation principle, the controller is designed with hierarchical inner-outer loop structure. The outer-loop position controller is constructed with hyperbolic tangent function, and temporary-path generation method is developed to keep the control matrix invertible and obviate large control energy. The desired command attitude can be derived from position controller without singularity by choosing appropriate controller parameters. The inner-loop attitude controller is designed with the unit-quaternion attitude representation and backstepping technique to achieve attitude tracking. Numerical simulation is provided to verify the theoretical results.

Keywords Miniature unmanned helicopter · Path following · Singularity-free control · Quaternion

1 Introduction

Tracking tasks for aircrafts can be classified as two categories [1]: trajectory tracking and path following. In the first case, the aircraft is required to track a time-varying reference trajectory at every transient. While in the second case it is required to fly along a reference path at a desired speed. Unlike trajectory tracking, there is no temporal requirements on path following. Besides the path following has some control performances that can not be obtained from trajectory tracking in some specific cases [2].

X. Ma · W. Huo (✉)
The Seventh Research Division, School of Automation Science
and Electrical Engineering, Beihang University, Beijing 100191, PR China
e-mail: weihuo@buaa.edu.cn

X. Ma
e-mail: maxujie@buaa.edu.cn

Y. Jia et al. (eds.), *Proceedings of 2017 Chinese Intelligent Systems Conference*,
Lecture Notes in Electrical Engineering 460,
https://doi.org/10.1007/978-981-10-6499-9_64

Various linear and nonlinear controllers have been proposed for path following control of miniature helicopters. The linear control methods are simple and reliable, such as PID [3] and LQ control [4, 5], but have the limitation to realize full envelope flight. To this end, some nonlinear control methods such as backstepping approach [6], feedback linearization technique [7] or hybrid control methods [8, 9] have been applied. Due to the under-actuated property, the helicopter model is always simplified to position outer-loop and attitude inner-loop structure [10, 11]. However, the controller designed based on the hierarchical structure may suffer from singularity when deriving the desired attitude from position controller. So far, only a few literatures [6] take into account this problem, and most reference paths are parameterized curves.

The parameterized path following [6, 8, 9] is the most commonly used problem formulation. The path is described with a time-varying parameter, and the task is to design control law and parameter timing law such that helicopter can keep up with the moving point determined by the parameter. Another problem formulation is based on implicit expressions [1, 7]. The path is given by the intersection of two manifolds. Unlike parameterized path following which turns path following problem to point-tracking problem, the task for implicit path following is to follow the entire path and the helicopter will enter an invariant set around the reference path. However, controller design for implicit path following always relates to control matrix of the closed-loop system, and it suffers from singularity when the matrix is not invertible.

In this paper a singularity-free implicit path following controller for miniature helicopters is presented. The control design is based on the hierarchical structure. The outer-loop position controller is constructed with the hyperbolic tangent function to realize path following, and a temporary path is planned to guarantee the control matrix invertible. From the position controller, the desired command attitude can be derived without singularity by choosing appropriate controller parameters. The inner-loop attitude controller is designed with the unit-quaternion representation to realize tracking for the command attitude.

2 Preliminaries

In following sections, $c(\cdot)$ and $s(\cdot)$ are shorts of $\cos(\cdot)$ and $\sin(\cdot)$. $|\cdot|$denotes absolute value of a real number, $\|\cdot\|$ denotes Euclidean norm for a vector or induced Euclidean norm for a matrix. $\bar{\lambda}(\cdot)$ and $\underline{\lambda}(\cdot)$ denote the maximum and minimum eigenvalues, respectively. For $\boldsymbol{x} = [x_1, \ldots, x_n]^T \in \mathbb{R}^n$, define hyperbolic tangent function vector $\tanh(\boldsymbol{x}) = [\tanh(x_1), \ldots, \tanh(x_n)]^T$ and hyperbolic tangent function matrix $\mathrm{Tanh}(\boldsymbol{x}) = \mathrm{diag}\{\tanh(x_1), \ldots, \tanh(x_n)\}$. For a continuously differentiable scalar function $f(\boldsymbol{x})$, define $\partial_{x_i} f = \frac{\partial f}{\partial x_i}(i = 1, \ldots n)$ and $\partial_{\boldsymbol{x}} f = [\frac{\partial f}{\partial x_1}, \ldots, \frac{\partial f}{\partial x_n}]^T$. For continuously differentiable vector function $\boldsymbol{f}(\boldsymbol{x}) = [f_1(\boldsymbol{x}), \ldots, f_m(\boldsymbol{x})]^T$, define $\partial_{\boldsymbol{x}}\boldsymbol{f} = \begin{bmatrix} \frac{\partial f_1}{\partial x_1} & \cdots & \frac{\partial f_1}{\partial x_n} \\ \vdots & \ddots & \vdots \\ \frac{\partial f_m}{\partial x_1} & \cdots & \frac{\partial f_m}{\partial x_n} \end{bmatrix}$ and $\partial^2_{\boldsymbol{x}} f = \partial_{\boldsymbol{x}}(\partial_{\boldsymbol{x}} f)$.

Lemma 1 ([12]) *For $x \in \mathbb{R}^n$, if $\|\boldsymbol{x}\| < \bar{x} < \infty$, then there exists a constant $\chi(\bar{x}) \in (0, 1)$ satisfying $\chi\|\boldsymbol{x}\| \le \|\tanh(\boldsymbol{x})\| \le \|\boldsymbol{x}\|$.*

Lemma 2 ([13]) *For $x \in \mathbb{R}$ and $\varepsilon > 0$, $0 \le |x| - x\tanh(x/\varepsilon) \le k_q\varepsilon$, where $k_q = 0.2785$ satisfies $k_q = e^{-(k_q+1)}$.*

Lemma 3 ([14]) *Given a smooth function $\beta(t) : \mathbb{R}^+ \to \mathbb{R}$, its derivatives can be estimated by the command filter $\ddot{x} = -2\xi\omega_n\dot{x} - \omega_n^2(x - \beta)$ such that $\dot{\beta} \approx \dot{x}, \ddot{\beta} \approx \ddot{x}$, where $\omega_n > 0$ is chosen large enough to ensure estimation accuracy.*

3 Problem Statement

Mathematical modeling Figure 1 shows the helicopter configuration, it is modeled in two frames: the earth frame $\mathcal{I} = \{Oxyz\}$ and fuselage frame $\mathcal{B} = \{O_b x_b y_b z_b\}$. Frame $\mathcal{I}$ is fixed to the earth and its origin locates on the ground. Frame $\mathcal{B}$ is fixed to the helicopter body and its origin locates at the helicopter center of gravity (c.g.). The rotation matrix R [1], which defines the rotation from $\mathcal{B}$ to $\mathcal{I}$ around an unit vector $\hat{\boldsymbol{k}} \in \mathbb{R}^3$ by an angle φ, is mostly used to describe attitude of the helicopter. The unit-quaternion $Q = [\mu, \boldsymbol{q}^T]^T = \{Q \in \mathbb{R} \times \mathbb{R}^3 | \mu^2 + \boldsymbol{q}^T\boldsymbol{q} = 1\}$ [15] can also be used to describe attitude, where $\mu = \cos\frac{\varphi}{2}$ and $\boldsymbol{q} = [q_1, q_2, q_3]^T = \sin\frac{\varphi}{2}\hat{\boldsymbol{k}}$. R and Q satisfy following relation

$$R(Q) = (\mu^2 - \boldsymbol{q}^T\boldsymbol{q})I_3 + 2\boldsymbol{q}\boldsymbol{q}^T + 2\mu S(\boldsymbol{q}) \tag{1}$$

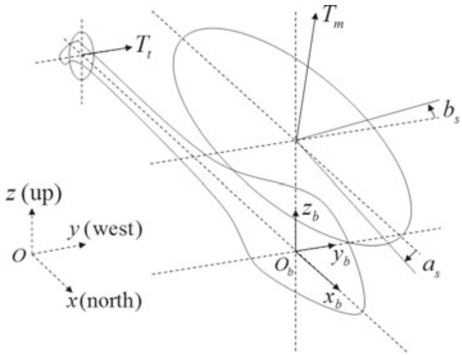

Fig. 1 Helicopter model and frames

where I_3 is 3×3 identity matrix, $S(\boldsymbol{q}) = \begin{bmatrix} 0 & -q_3 & q_2 \\ q_3 & 0 & -q_1 \\ -q_2 & q_1 & 0 \end{bmatrix}$. Given $Q_1 = \begin{bmatrix} \mu_1 \\ \boldsymbol{q_1} \end{bmatrix}$ and $Q_2 = \begin{bmatrix} \mu_2 \\ \boldsymbol{q_2} \end{bmatrix}$, the quaternion multiplication $Q_1 \otimes Q_2 = \begin{bmatrix} \mu_1\mu_2 - \boldsymbol{q_1}^T\boldsymbol{q_2} \\ \mu_1\boldsymbol{q_2} + \mu_2\boldsymbol{q_1} + S(\boldsymbol{q_1})\boldsymbol{q_2} \end{bmatrix}$. The inverse of Q is defined as $Q^{-1} = [\mu, -\boldsymbol{q}^T]^T$ and satisfies $Q^{-1} \otimes Q = [1, 0, 0, 0]^T$.

Based on the Newton–Euler equations, the dynamic model of the helicopter can be derived as follows [1]

$$\dot{\boldsymbol{p}} = \boldsymbol{v}, \quad m\dot{\boldsymbol{v}} = -m\boldsymbol{g_3} + R(Q)\boldsymbol{f} \tag{2}$$

$$\dot{Q} = \frac{1}{2}\Theta(Q)\boldsymbol{\omega}, \quad J\dot{\boldsymbol{\omega}} = -\boldsymbol{\omega} \times J\boldsymbol{\omega} + \boldsymbol{\tau} \tag{3}$$

where $\boldsymbol{p} = [x, y, z]^T$ and $\boldsymbol{v} = [u, v, w]^T$ are position and velocity of helicopter denoted in $\mathcal{I}$, m is the helicopter mass, $\boldsymbol{g_3} = [0, 0, g]^T$ and g is gravitational acceleration, $\boldsymbol{\omega} = [\omega_x, \omega_y, \omega_z]^T$ is angular velocity denoted in $\mathcal{B}$, $\Theta(Q) = \begin{bmatrix} -\boldsymbol{q}^T \\ \mu I_3 + S(\boldsymbol{q}) \end{bmatrix}$ is attitude transition matrix, $J = \begin{bmatrix} J_x & 0 & -J_{xz} \\ 0 & J_y & 0 \\ -J_{xz} & 0 & J_z \end{bmatrix}$ is the inertial matrix denoted in $\mathcal{B}$. The applied force $\boldsymbol{f}$ and torque $\boldsymbol{\tau}$ denoted in $\mathcal{B}$ are given by [1]

$$\boldsymbol{f} = \begin{bmatrix} T_m sa_s cb_s \\ -T_m sb_s ca_s + T_t \\ T_m ca_s cb_s \end{bmatrix}, \boldsymbol{\tau} = \begin{bmatrix} T_m h_m sb_s + L_b b_s + T_t h_t + \tau_m sa_s \\ T_m l_m + T_m h_m sa_s + M_a a_s + \tau_t - \tau_m sb_s \\ -T_m l_m sb_s - T_t l_t + \tau_m ca_s cb_s \end{bmatrix} \tag{4}$$

where T_m, τ_m, T_t, τ_t are thrust and anti-torque generated by the main and tail rotors, respectively; M_a, L_b are stiffness coefficients of main rotor; h_m, h_t, l_m, l_t denote vertical and horizontal distances between the rotor centers and helicopter c.g.; a_s, b_s denote longitudinal and lateral flapping angles of the main rotor. The relationship between thrusts T_i and anti-torque τ_i ($i = m$ or t) is given by [12]

$$\tau_i = A_i|T_i|^{1.5} + B_i \tag{5}$$

where A_i and B_i are aerodynamic constants.

Due to the limitation of helicopter physical structure, a_s, b_s, T_t and τ_t are fairly small, thus it is reasonable to express (4) as [11]:

$$\boldsymbol{f} = [0, 0, T_m]^T + \boldsymbol{f}_\Delta, \ \boldsymbol{\tau} = Q_A\boldsymbol{\rho} + \boldsymbol{\tau}_B + \boldsymbol{\Delta}_\tau = \boldsymbol{\tau}_1 + \boldsymbol{\Delta}_\tau \tag{6}$$

where $\boldsymbol{\rho} = \begin{bmatrix} T_t \\ a_s \\ b_s \end{bmatrix}$, $\boldsymbol{\tau}_B = \begin{bmatrix} 0 \\ T_m l_m \\ \tau_m \end{bmatrix}$, $Q_A = \begin{bmatrix} h_t & \tau_m & T_m h_m + L_b \\ 0 & T_m h_m + M_a & -\tau_m \\ -l_t & 0 & -T_m l_m \end{bmatrix}$ and $\det(Q_A) \neq 0$ [1]; $\boldsymbol{f}_\Delta$ and $\boldsymbol{\Delta}_\tau$ are bounded and small [12]. The real input $\boldsymbol{\rho} = Q_A^{-1}(\boldsymbol{\tau}_1 - \boldsymbol{\tau}_B)$. Equation (2) can be rewritten as

$$\dot{\boldsymbol{v}} = -\boldsymbol{g_3} + (T_m/m)\boldsymbol{r}_3 + \bar{\boldsymbol{f}}_\Delta \tag{7}$$

where $\boldsymbol{r_3} = R\boldsymbol{e_3}$, $\boldsymbol{e}_3 = [0, 0, 1]^T$, $\bar{\boldsymbol{f}}_\Delta = \frac{1}{m}R\boldsymbol{f}_\Delta$.

Control objective The reference path $\mathcal{P}_r$ is a regular curve described by implicit expressions, i.e. $\mathcal{P}_r = \{[x, y, z]^T | f_1(x, y, z) = 0, f_2(x, y, z) = 0\}$, and $\partial_{\boldsymbol{p}} f_1 \times \partial_{\boldsymbol{p}} f_2|_{\boldsymbol{p}\in\mathcal{P}_r} \neq 0$, where $f_1, f_2 \in C^\infty$; $\|\partial_{\boldsymbol{p}} f_1\|, \|\partial_{\boldsymbol{p}} f_2\|$ are bounded on $\mathcal{P}_r$. In this paper the manifold $f_1 = 0$ is specified as a plane $f_1 = ax + by + cz + d = 0$.

Remark 1 From $f_1, f_2 \in C^\infty$ it follows that $\partial_{\boldsymbol{p}} f_1 \times \partial_{\boldsymbol{p}} f_2 \in C^\infty$ and $\partial_{\boldsymbol{p}} f_1 \times \partial_{\boldsymbol{p}} f_2 \neq 0$ in neighbourhood of $\mathcal{P}_r$.

The control object is: (i) designing control inputs T_m, T_t, a_s, b_s such that the helicopter trajectory converges to the reference path ultimately and the magnitude of its velocity projection on reference path tends to desired speed $v_r > 0$, i.e. there exit small positive constants o_1, o_2, o_3 such that

$$\begin{aligned} &\lim_{t\to\infty} |f_1(x, y, z)| < o_1, \quad \lim_{t\to\infty} |f_2(x, y, z)| < o_2 \\ &\lim_{t\to\infty} \left| \left(\frac{\partial_{\boldsymbol{p}} f_1 \times \partial_{\boldsymbol{p}} f_2}{\|\partial_{\boldsymbol{p}} f_1 \times \partial_{\boldsymbol{p}} f_2\|} \right)^T \boldsymbol{v} - v_r \right| < o_3 \end{aligned} \tag{8}$$

(ii) No singularity occurs in control process.

4 Controller Design

Define the path-following and velocity errors

$$\varsigma_1 = f_1(x, y, z), \quad \varsigma_2 = f_2(x, y, z), \quad \varsigma_3 = \boldsymbol{\eta}^T \boldsymbol{v} - v_r \tag{9}$$

where $\boldsymbol{\eta} = \frac{\partial_{\boldsymbol{p}} f_1 \times \partial_{\boldsymbol{p}} f_2}{\|\partial_{\boldsymbol{p}} f_1 \times \partial_{\boldsymbol{p}} f_2\|}$, we can derive

$$[\dot{\varsigma}_1, \dot{\varsigma}_2, \varsigma_3]^T = G\boldsymbol{v} - [0, 0, v_r]^T, \quad [\ddot{\varsigma}_1, \ddot{\varsigma}_2, \dot{\varsigma}_3]^T = \boldsymbol{h} + G\dot{\boldsymbol{v}} \tag{10}$$

where $\boldsymbol{h} = [0, \boldsymbol{v}^T(\partial^2_{\boldsymbol{p}} f_2)\boldsymbol{v}, \boldsymbol{v}^T(\partial_{\boldsymbol{p}}\boldsymbol{\eta})\boldsymbol{v} - \dot{v}_r]^T$, $G = [\partial_{\boldsymbol{p}} f_1, \partial_{\boldsymbol{p}} f_2, \boldsymbol{\eta}]^T$ is the control matrix. From (10) and (7) we know

$$[\ddot{\varsigma}_1, \ddot{\varsigma}_2, \dot{\varsigma}_3]^T = \boldsymbol{h} + G[-\boldsymbol{g_3} + (T_m/m)\boldsymbol{r_3}] + \boldsymbol{\Delta}_f \tag{11}$$

where $\boldsymbol{\Delta}_f = G\bar{\boldsymbol{f}}_\Delta$. Define the position loop controller $\boldsymbol{u_c} = T_m\boldsymbol{r_3}$ and design

$$\boldsymbol{u_c} = [u_{cx}, u_{cy}, u_{cz}]^T = m(\boldsymbol{g_3} + G^{-1}(-\boldsymbol{h} + \boldsymbol{v}_c)) \tag{12}$$

Fig. 2 Temporary path generator

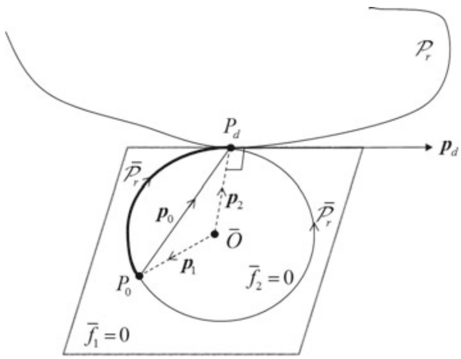

where $\boldsymbol{v}_c$ is a new control input to be determined. The singularity occurs when $\det(G) = (\partial_{\boldsymbol{p}} f_1 \times \partial_{\boldsymbol{p}} f_2)^T \boldsymbol{\eta} = \|\partial_{\boldsymbol{p}} f_1 \times \partial_{\boldsymbol{p}} f_2\| = 0$. From Remark 1, G is invertible in neighborhood of $\mathcal{P}_r$. When helicopter initial position is far from $\mathcal{P}_r$, G cannot be guaranteed to be invertible. Besides, when helicopter is far from the path, the control energy will be large. A solution for the two problems is to plan a temporary path $\bar{\mathcal{P}}_r$ from initial position to $\mathcal{P}_r$ such that corresponding control matrix $\bar{G}$ is invertible on $\bar{\mathcal{P}}_r$. In this paper define P_0 to be the initial position, when $\sqrt{|f_1(P_0)|^2 + |f_2(P_0)|^2} > 10$, it is need to plan a temporary-path.

Assumption 1 $\boldsymbol{\Delta}_f = [\Delta_{fx}, \Delta_{fy}, \Delta_{fz}]^T$ and $\boldsymbol{\Delta}_\tau = [\Delta_{\tau x}, \Delta_{\tau y}, \Delta_{\tau z}]^T$ are bounded and satisfy $|\Delta_{fi}| \le \delta_i, |\Delta_{\tau i}| \le \gamma_i$ $(i = x, y, z)$, where $\boldsymbol{\delta} = [\delta_x, \delta_y, \delta_z]^T$ and $\boldsymbol{\gamma} = [\gamma_x, \gamma_y, \gamma_z]^T$ are known upper bounds; The coefficient c in $f_1 = 0$ satisfies $|c| > \delta_x/g$ for avoiding singularity in deriving desired unit-quaternion. The physical meaning is that $f_1 = 0$ is not perpendicular to $x - y$ plane of $\mathcal{I}$.

Path planning As illustrated in Fig. 2, the initial position $P_0 = [x_0, y_0, z_0]^T$. Choose a point $P_d = [x_r, y_r, z_r]^T$ on $\mathcal{P}_r$ and compute tangent vector $\boldsymbol{p}_d = [\bar{x}, \bar{y}, \bar{z}]^T = \partial_{\boldsymbol{p}} f_1 \times \partial_{\boldsymbol{p}} f_2|_{P_d}$. Define $\boldsymbol{p}_0 = \overrightarrow{P_0 P_d}$ and compute $\boldsymbol{p}_0 \times \boldsymbol{p}_d = [\bar{x}_1, \bar{y}_1, \bar{z}_1]^T$. If P_d are chosen such that $\bar{z}_1 \ne 0$ and $\boldsymbol{p}_0$ is not collinear with $\boldsymbol{p}_d$, a temporary path can be planned with following steps:

Firstly, passing through $\boldsymbol{p}_0$ and $\boldsymbol{p}_d$ we can define a plane $\bar{f}_1 = a_1 x + b_1 y + c_1 z + d_1 = 0$. Since P_d lies on $\bar{f}_1 = 0$ and its normal vector is $\boldsymbol{p}_0 \times \boldsymbol{p}_d$, we know $d_1 = -a_1 x_r - b_1 y_r - c_1 z_r$ and $[a_1, b_1, c_1] = k[\bar{x}_1, \bar{y}_1, \bar{z}_1]$, where k is a constant. Considering $\bar{z}_1 \ne 0$, choosing $|k| > \frac{\delta_x}{|\bar{z}_1| g}$ can guarantee that $c_1 > \delta_x/g$.

Then, define $\bar{f}_2 = 0$ to be a sphere, its center $\bar{O} = [a_2, b_2, c_2]^T$, $\boldsymbol{p}_1 = \overrightarrow{\bar{O} P_0}$ and $\boldsymbol{p}_2 = \overrightarrow{\bar{O} P_d}$. Since $\boldsymbol{p}_2 \perp \boldsymbol{p}_d$, $\bar{f}_1(\bar{O}) = 0$ and $\|\boldsymbol{p}_1\| = \|\boldsymbol{p}_2\|$, $\bar{O}$ can be determined by

$$\begin{bmatrix} a_2 \\ b_2 \\ c_2 \end{bmatrix} = \begin{bmatrix} \bar{x} & \bar{y} & \bar{z} \\ a_1 & b_1 & c_1 \\ x_r - x_0 & y_r - y_0 & z_r - z_0 \end{bmatrix}^{-1} \begin{bmatrix} \bar{x} x_r + \bar{y} y_r + \bar{z} z_r \\ -d_1 \\ \frac{x_r^2 - x_0^2 + y_r^2 - y_0^2 + z_r^2 - z_0^2}{2} \end{bmatrix}$$

Since $\boldsymbol{p}_0$ is not collinear to $\boldsymbol{p}_d$, above inverse matrix is well defined and $[a_2, b_2, c_2]^T$ can be determined uniquely. Define $\|\boldsymbol{p}_1\| = r$, we have $\bar{f}_2 = \frac{1}{k_1}((x-a_2)^2 + (y-b_2)^2 + (z-c_2)^2 - r^2) = 0$, where $k_1 \neq 0$ is a constant.

Finally, temporary path $\bar{\mathcal{P}}_r$ is the intersection of $\bar{f}_1 = 0$ and $\bar{f}_2 = 0$. Since two paths are generated (bold line and normal one in Fig. 2), the one with smaller angle from its tangent line at P_0 to helicopter head direction should be selected.

Remark 2 $\bar{\mathcal{P}}_r$ satisfies that 1) $\partial_{\boldsymbol{p}}\bar{f}_1 \times \partial_{\boldsymbol{p}}\bar{f}_2$ is collinear with $\partial_{\boldsymbol{p}} f_1 \times \partial_{\boldsymbol{p}} f_2$ at P_d. 2) $\partial_{\boldsymbol{p}}\bar{f}_1 \perp \partial_{\boldsymbol{p}}\bar{f}_2$ on $\bar{\mathcal{P}}_r$, i.e. $\partial_{\boldsymbol{p}}\bar{f}_1 \times \partial_{\boldsymbol{p}}\bar{f}_2 \neq 0$ on $\bar{\mathcal{P}}_r$. Since $\bar{f}_1, \bar{f}_2 \in C^\infty$, it holds near $\bar{\mathcal{P}}_r$, i.e. control matrix $\bar{G}$ invertible near $\bar{\mathcal{P}}_r$.

$\bar{\mathcal{P}}_{\mathbf{r}}$ following The position loop controller design is divided to two steps: $\bar{\mathcal{P}}_r$ following and then $\mathcal{P}_r$ following. Firstly define errors for the temporary path $\bar{\mathcal{P}}_r$

$$\begin{aligned}
&\bar{\varsigma}_1 = a_1 x + b_1 y + c_1 z + d_1, \quad \bar{\varsigma}_2 = \frac{1}{k_1}((x-a_2)^2 + (y-b_2)^2 + (z-c_2)^2 - r^2) \\
&\bar{\varsigma}_3 = \bar{\boldsymbol{\eta}}^T \boldsymbol{v} - \bar{v}_r
\end{aligned} \tag{13}$$

where $\bar{\boldsymbol{\eta}} = \frac{\bar{\boldsymbol{\eta}}_1 \times \bar{\boldsymbol{\eta}}_2}{\|\bar{\boldsymbol{\eta}}_1 \times \bar{\boldsymbol{\eta}}_2\|}$, $\bar{\boldsymbol{\eta}}_1 = [a_1, b_1, c_1]^T$, $\bar{\boldsymbol{\eta}}_2 = \frac{2}{k_1}[x-a_2, y-b_2, z-c_2]^T$. It yields

$$[\dot{\bar{\varsigma}}_1, \dot{\bar{\varsigma}}_2, \bar{\varsigma}_3]^T = \bar{G}\boldsymbol{v} - [0, 0, \bar{v}_r]^T \tag{14}$$

$$[\ddot{\bar{\varsigma}}_1, \ddot{\bar{\varsigma}}_2, \dot{\bar{\varsigma}}_3]^T = \bar{\boldsymbol{h}} + \bar{G}[-\boldsymbol{g}_3 + (T_m/m)\boldsymbol{r}_3] + \boldsymbol{\Delta}_f \tag{15}$$

where $\bar{G} = [\bar{\boldsymbol{\eta}}_1, \bar{\boldsymbol{\eta}}_2, \bar{\boldsymbol{\eta}}]^T$ is control matrix, $\bar{\boldsymbol{h}} = [\bar{h}_1, \bar{h}_2, \bar{h}_3]^T = [0, \frac{2}{k_1}\boldsymbol{v}^T\boldsymbol{v}, \boldsymbol{v}^T(\partial_{\boldsymbol{p}}\bar{\boldsymbol{\eta}})\boldsymbol{v} - \dot{\bar{v}}_r]^T$. Define $\bar{\boldsymbol{u}}_c = T_m \boldsymbol{r}_3$ and design it as

$$\bar{\boldsymbol{u}}_c = [\bar{u}_{cx}, \bar{u}_{cy}, \bar{u}_{cz}]^T = m(\boldsymbol{g}_3 + \bar{G}^{-1}(-\bar{\boldsymbol{h}} + \bar{\boldsymbol{v}}_c)) \tag{16}$$

$$\bar{\boldsymbol{v}}_c = \begin{bmatrix} \bar{v}_1 \\ \bar{v}_2 \\ \bar{v}_3 \end{bmatrix} = \begin{bmatrix} -\bar{k}_{11}(\tanh(\bar{\varsigma}_{k1}) + \tanh(\dot{\bar{\varsigma}}_1)) - \tanh(\frac{\bar{\vartheta}_1}{\bar{\varepsilon}_1})\delta_x \\ -\bar{k}_{21}(\tanh(\bar{\varsigma}_{k2}) + \tanh(\dot{\bar{\varsigma}}_2)) - \tanh(\frac{\bar{\vartheta}_2}{\bar{\varepsilon}_2})\delta_y \\ -\bar{k}_{31}\tanh(\bar{\varsigma}_3) - \tanh(\frac{\bar{\varsigma}_3}{\bar{\varepsilon}_3})\delta_z \end{bmatrix} \tag{17}$$

where $\bar{\varsigma}_{k1} = \bar{k}_{12}\bar{\varsigma}_1 + \dot{\bar{\varsigma}}_1$, $\bar{\varsigma}_{k2} = \bar{k}_{22}\bar{\varsigma}_2 + \dot{\bar{\varsigma}}_2$, $\bar{\vartheta}_1 = \tanh(\bar{\varsigma}_{k1}) + \tanh(\dot{\bar{\varsigma}}_1) + \frac{\bar{k}_{12}}{\bar{k}_{11}}\dot{\bar{\varsigma}}_1$, $\bar{\vartheta}_2 = \tanh(\bar{\varsigma}_{k2}) + \tanh(\dot{\bar{\varsigma}}_2) + \frac{\bar{k}_{22}}{\bar{k}_{21}}\dot{\bar{\varsigma}}_2$; $\bar{k}_{11}, \bar{k}_{12}, \bar{k}_{21}, \bar{k}_{22}, \bar{k}_{31}, \bar{\varepsilon}_1, \bar{\varepsilon}_2, \bar{\varepsilon}_3$ are positive constants. Since $\|\boldsymbol{r}_3\| = 1$, $T_m = \|\bar{\boldsymbol{u}}_c\|$. If $\bar{\boldsymbol{u}}_c \notin \mathcal{L} = \{[0, 0, u]^T, u \leq 0\}$, then the desired unit-quaternion $Q_c = [\mu_c, \boldsymbol{q}_c^T]^T$ can be derived from $\bar{\boldsymbol{u}}_c$ [12]

$$\boldsymbol{q}_c = \frac{1}{2\|\bar{\boldsymbol{u}}_c\|\mu_c} \begin{bmatrix} \bar{u}_{cy} \\ -\bar{u}_{cx} \\ 0 \end{bmatrix}, \mu_c = \sqrt{\frac{\|\bar{\boldsymbol{u}}_c\| + \bar{u}_{cz}}{2\|\bar{\boldsymbol{u}}_c\|}} \tag{18}$$

Theorem 1 *If initial velocity* $\boldsymbol{v}(0) = \mathbf{0}$ *and the parameters in* (17) *satisfy*

$$\bar{k}_{12} \leq \bar{k}_{11} < \frac{|c_1|g - \delta_x}{2}, \bar{k}_{22} \leq \bar{k}_{21}, \bar{\varepsilon}_1 < \frac{0.382\bar{k}_{12}}{k_q\delta_x}, \bar{\varepsilon}_2 < \frac{0.382\bar{k}_{22}}{k_q\delta_y} \tag{19}$$

Then control law (16) *guarantees:* (*i*) $\bar{\varsigma}_1, \dot{\bar{\varsigma}}_1, \bar{\varsigma}_2, \dot{\bar{\varsigma}}_2, \bar{\varsigma}_3$ *are bounded and converge to a small neighbourhood of origin.* (*ii*) $\bar{G}$ *is invertible during control and no singularity occurs in deriving desired unit-quaternion with* (18).

Proof (*i*) Define $\bar{\boldsymbol{\varsigma}} = [\bar{\varsigma}_{k1}, \dot{\bar{\varsigma}}_1]$, choose Lyapunov function

$$V = \int_0^{\bar{\varsigma}_{k1}} \tanh(s)ds + \int_0^{\dot{\bar{\varsigma}}_1} \tanh(s)ds + \frac{\bar{k}_{12}}{2\bar{k}_{11}}\dot{\bar{\varsigma}}_1^2 \tag{20}$$

$$\begin{aligned} \dot{V} &= -\bar{k}_{11}[\tanh(\bar{\varsigma}_{k1}) + \tanh(\dot{\bar{\varsigma}}_1)]^2 - \bar{k}_{12}\dot{\bar{\varsigma}}_1\tanh(\dot{\bar{\varsigma}}_1) - \bar{\vartheta}_1[\tanh(\frac{\bar{\vartheta}_1}{\bar{\varepsilon}_1})\delta_x - \Delta_{fx}] \\ &\leq -\tanh^T(\bar{\boldsymbol{\varsigma}}) \begin{bmatrix} \bar{k}_{11} & \bar{k}_{11} \\ \bar{k}_{11} & \bar{k}_{11} + \bar{k}_{12} \end{bmatrix} \tanh(\bar{\boldsymbol{\varsigma}}) - \bar{\vartheta}_1\tanh(\frac{\bar{\vartheta}_1}{\bar{\varepsilon}_1})\delta_x + \bar{\vartheta}_1\Delta_{fx} \end{aligned} \tag{21}$$

Based on Lemma 2, we know $\bar{\vartheta}_1\Delta_{fx} \leq |\bar{\vartheta}_1|\delta_x \leq [\bar{\vartheta}_1\tanh(\frac{\bar{\vartheta}_1}{\bar{\varepsilon}_1}) + k_q\bar{\varepsilon}_1]\delta_x$. Considering $\begin{bmatrix} \bar{k}_{11} & \bar{k}_{11} \\ \bar{k}_{11} & \bar{k}_{11} + \bar{k}_{12} \end{bmatrix} = \Lambda^T \begin{bmatrix} \bar{k}_{11} & 0 \\ 0 & \bar{k}_{12} \end{bmatrix} \Lambda$, where $\Lambda = \begin{bmatrix} 1 & 1 \\ 0 & 1 \end{bmatrix}$, (21) yields $\dot{V} \leq k_q\bar{\varepsilon}_1\delta_x - \underline{\lambda}(\Lambda^T\Lambda)\min\{\bar{k}_{11}, \bar{k}_{12}\}\|\tanh(\bar{\boldsymbol{\varsigma}})\|^2 = k_q\bar{\varepsilon}_1\delta_x - 0.382\bar{k}_{12}\|\tanh(\bar{\boldsymbol{\varsigma}})\|^2$. From (19) we know $\frac{k_q\bar{\varepsilon}_1\delta_x}{0.382\bar{k}_{12}} < 1$. When $\|\tanh(\bar{\boldsymbol{\varsigma}})\| > \sqrt{\frac{k_q\bar{\varepsilon}_1\delta_x}{0.382\bar{k}_{12}}}$, $\dot{V} < 0$, which means $\bar{\boldsymbol{\varsigma}}$ is bounded. Then from Lemma 1 we have $\chi\|\bar{\boldsymbol{\varsigma}}\| \leq \|\tanh(\bar{\boldsymbol{\varsigma}})\|$, where $0 < \chi < 1$, it follows

$$\dot{V} \leq -0.382\bar{k}_{12}\chi^2\|\bar{\boldsymbol{\varsigma}}\|^2 + k_q\bar{\varepsilon}_1\delta_x \tag{22}$$

Besides, from (20) we have $\frac{\chi}{2}\|\bar{\boldsymbol{\varsigma}}\|^2 \leq V \leq \chi_2\|\bar{\boldsymbol{\varsigma}}\|^2$, where $\chi_2 = \frac{1}{2}(1 + \frac{\bar{k}_{12}}{\bar{k}_{11}})$. Then $\dot{V} \leq -\frac{0.382\bar{k}_{12}\chi^2}{\chi_2}V + k_q\bar{\varepsilon}_1\delta_x$. Integrating it yields

$$\frac{\chi}{2}\|\bar{\boldsymbol{\varsigma}}\|^2 \leq V \leq [V(0) - \frac{k_q\bar{\varepsilon}_1\delta_x\chi_2}{0.382\bar{k}_{12}\chi^2}]e^{\frac{-0.382\bar{k}_{12}\chi^2}{\chi_2}t} + \frac{k_q\bar{\varepsilon}_1\delta_x\chi_2}{0.382\bar{k}_{12}\chi^2} \tag{23}$$

So $\bar{\boldsymbol{\varsigma}}$ exponentially converges to the set $\mathbb{Z}_{v1} = \{\bar{\boldsymbol{\varsigma}} | \|\bar{\boldsymbol{\varsigma}}\| \leq \sqrt{\frac{0.73\bar{\varepsilon}_1\delta_x}{\chi^3}(\frac{1}{\bar{k}_{12}} + \frac{1}{\bar{k}_{11}})}\}$. Due that $|\dot{\bar{\varsigma}}_1| \leq \|\bar{\boldsymbol{\varsigma}}\|$, $\dot{\bar{\varsigma}}_1$ also converges to $\mathbb{Z}_{v1}$. Considering $\dot{\bar{\varsigma}}_1 = -\bar{k}_{12}\bar{\varsigma}_1 + \bar{\varsigma}_{k1}$ and $|\bar{\varsigma}_{k1}| \leq \|\bar{\boldsymbol{\varsigma}}\|$, integrating $\dot{\bar{\varsigma}}_1$ yields

$$|\bar{\varsigma}_1| \le e^{-\bar{k}_{12}t}(|\bar{\varsigma}_1(0)| - \sqrt{\frac{2k_q\bar{\varepsilon}_1\delta_x\chi_2}{0.382\bar{k}_{12}^3\chi^3}}) + \sqrt{\frac{2k_q\bar{\varepsilon}_1\delta_x\chi_2}{0.382\bar{k}_{12}^3\chi^3}} \tag{24}$$

Thus $\bar{\varsigma}_1$ converges to set $\mathbb{Z}_{p1} = \{|\bar{\varsigma}_1| \le \frac{1}{\bar{k}_{12}}\sqrt{\frac{0.73\bar{\varepsilon}_1\delta_x}{\chi^3}(\frac{1}{\bar{k}_{12}} + \frac{1}{\bar{k}_{11}})}\}$. Similarly, $\bar{\varsigma}_2$ and $\dot{\bar{\varsigma}}_2$ exponentially converge to sets $\mathbb{Z}_{p2} = \{\bar{\varsigma}_2||\bar{\varsigma}_2| \le \frac{1}{\bar{k}_{22}}\sqrt{\frac{0.73\bar{\varepsilon}_2\delta_y}{\chi^3}(\frac{1}{\bar{k}_{22}} + \frac{1}{\bar{k}_{21}})}\}$ and $\mathbb{Z}_{v2} = \{\dot{\bar{\varsigma}}_2||\dot{\bar{\varsigma}}_2| \le \sqrt{\frac{0.73\bar{\varepsilon}_2\delta_y}{\chi^3}(\frac{1}{\bar{k}_{22}} + \frac{1}{\bar{k}_{21}})}\}$, respectively.

For $\bar{\varsigma}_3$, choose Lyapunov function $V_1 = \frac{1}{2}\bar{\varsigma}_3^2$, its derivative is

$$\dot{V}_1 = -\bar{k}_{31}\bar{\varsigma}_3\tanh(\bar{\varsigma}_3) - \bar{\varsigma}_3\tanh\left(\frac{\bar{\varsigma}_3}{\bar{\varepsilon}_3}\right)\delta_z + \bar{\varsigma}_3\Delta_{fz} \tag{25}$$

From Lemma 2, $\bar{\varsigma}_3\Delta_{fz} \le |\bar{\varsigma}_3|\delta_z \le (\bar{\varsigma}_3\tanh(\frac{\bar{\varsigma}_3}{\bar{\varepsilon}_3}) + k_q\bar{\varepsilon}_3)\delta_z$, thus $\dot{V}_1 \le -\bar{k}_{31}\bar{\varsigma}_3\tanh(\bar{\varsigma}_3) + k_q\bar{\varepsilon}_3\delta_z$. Based on Lemma 1 we have $\dot{V}_1 \le -\bar{k}_{31}\chi\bar{\varsigma}_3^2 + k_q\bar{\varepsilon}_3\delta_z = -2\bar{k}_{31}\chi V_1 + k_q\bar{\varepsilon}_3\delta_z$. Integrating it yields

$$\frac{1}{2}\bar{\varsigma}_3^2 = V_1(t) \le [V_1(0) - \frac{k_q\bar{\varepsilon}_3\delta_z}{2\bar{k}_{31}\chi}]e^{-2\bar{k}_{31}\chi t} + \frac{k_q\bar{\varepsilon}_3\delta_z}{2\bar{k}_{31}\chi} \tag{26}$$

Thus $\bar{\varsigma}_3$ exponentially converges to the set $\mathbb{Z}_3 = \{\bar{\varsigma}_3||\bar{\varsigma}_3| \le \sqrt{\frac{0.2785\bar{\varepsilon}_3\delta_z}{\bar{k}_{31}\chi}}\}$.

Above sets can be made small by increasing $\bar{k}_{21}, \bar{k}_{22}, \bar{k}_{31}$ and decreasing $\bar{\varepsilon}_1, \bar{\varepsilon}_2, \bar{\varepsilon}_3$. Since $\boldsymbol{p}(0) \in \bar{\mathcal{P}}_r$ and $\boldsymbol{v}(0) = \boldsymbol{0}$, we have $\bar{\varsigma}_1(0) = \dot{\bar{\varsigma}}_1(0) = \bar{\varsigma}_2(0) = \dot{\bar{\varsigma}}_2(0) = 0$. So under the control law helicopter keeps in the neighbourhood of $\bar{\mathcal{P}}_r$.

(ii) From Remark 2 and proof of (i) it yields that $\bar{G}$ keeps invertible. When $\bar{u}_{cx} \ne 0$ or $\bar{u}_{cy} \ne 0$, $\bar{\boldsymbol{u}}_c \notin \mathcal{L}$, which means no singularity occurs in deriving the desired unit-quaternion. So we only need to consider the singularity when $\bar{\boldsymbol{u}}_c = [0, 0, \bar{u}_{cz}]^T$. Left-multiplying (16) by $[a_1, b_1, c_1]$ yields $\bar{u}_{cz} = m(g + \frac{\bar{v}_1}{c_1})$. From (17) $|\frac{\bar{v}_1}{c_1}| \le \frac{2\bar{k}_{11}+\delta_x}{|c_1|}$, it follows $\bar{u}_{cz} \ge m(g - \frac{2\bar{k}_{11}+\delta_x}{|c_1|})$. Since $\bar{k}_{11} < \frac{|c_1|g-\delta_x}{2}$, we get $\bar{u}_{cz} > 0$ and $\bar{\boldsymbol{u}}_c \notin \mathcal{L}$, which means no singularity occurs in deriving the desired unit-quaternion with (18).

$\mathcal{P}_\mathbf{r}$ **following** Define P to be helicopter position and $\bar{\varepsilon}$ to be a small positive constant, when $\|P - P_d\| \le \bar{\varepsilon}$, control $\boldsymbol{u}_c$ is given by (12) and $\boldsymbol{v}_c$ is designed as

$$\boldsymbol{v}_c = \begin{bmatrix} -k_{11}(\tanh(\varsigma_{k1}) + \tanh(\dot{\varsigma}_1)) - \tanh(\frac{\vartheta_1}{\varepsilon_1})\delta_x \\ -k_{21}(\tanh(\varsigma_{k2}) + \tanh(\dot{\varsigma}_2)) - \tanh(\frac{\vartheta_2}{\varepsilon_2})\delta_y \\ -k_{31}\tanh(\varsigma_3) - \tanh(\frac{\varsigma_3}{\varepsilon_3})\delta_z \end{bmatrix} \tag{27}$$

where $\varsigma_{k1} = k_{12}\varsigma_1 + \dot{\varsigma}_1$, $\varsigma_{k2} = k_{22}\varsigma_2 + \dot{\varsigma}_2$, $\vartheta_1 = \tanh(\varsigma_{k1}) + \tanh(\dot{\varsigma}_1) + \frac{k_{12}}{k_{11}}\dot{\varsigma}_1$, $\vartheta_2 = \tanh(\varsigma_{k2}) + \tanh(\dot{\varsigma}_2) + \frac{k_{22}}{k_{21}}\dot{\varsigma}_2$. $k_{11}, k_{12}, k_{21}, k_{22}, k_{31}, \varepsilon_1, \varepsilon_2$ and ε_3 are positive constants satisfying

$$k_{12} \leq k_{11} < \frac{|c|g - \delta_x}{2}, k_{22} \leq k_{21}, \varepsilon_1 < \frac{0.382k_{12}}{k_q\delta_x}, \varepsilon_2 < \frac{0.382k_{22}}{k_q\delta_y} \tag{28}$$

From Remark 2, $\boldsymbol{v}$ is approximately tangent to $\mathcal{P}_r$ at switching instant. So under the control law helicopter keeps in the neighbourhood of $\mathcal{P}_r$. Based on Remark 1 it yields that G keeps invertible. The constraint for k_{11} in (28) guarantees that no singularity occurs in deriving desired unit-quaternion.

Attitude controller design Define attitude tracking error $Q_e = [\mu_e, \boldsymbol{q}_e^T]^T = Q_c^{-1} \otimes Q$ [15], its derivative is

$$\dot{\mu}_e = -\frac{1}{2}\boldsymbol{q}_e^T\boldsymbol{\omega}_e,\ \dot{\boldsymbol{q}}_e = \frac{1}{2}(\mu_e I_3 + S(\boldsymbol{q}_e))\boldsymbol{\omega}_e \tag{29}$$

where $\boldsymbol{\omega}_e = \boldsymbol{\omega} - R^T(Q_e)\boldsymbol{\omega}_c$ is the angular velocity error and $\boldsymbol{\omega}_c$ is the desired angular velocity. From (3) $\boldsymbol{\omega}_c$ and its derivative $\dot{\boldsymbol{\omega}}_c$ can be derived as

$$\boldsymbol{\omega}_c = 2\Theta^T(Q_c)\dot{Q}_c \tag{30}$$

$$\dot{\boldsymbol{\omega}}_c = 2\Theta^T(Q_c)\ddot{Q}_c + 2\dot{\Theta}^T(Q_c)\dot{Q}_c = 2\Theta^T(Q_c)[\ddot{Q}_c - \dot{\Theta}_c\boldsymbol{\omega}_c] \tag{31}$$

where $\dot{\Theta}_c = \Theta(\dot{Q}_c)$. From Lemma 3, $\dot{Q}_c$ and $\ddot{Q}_c$ can be obtained by a command filter instead of calculating them accurately. Assign Lyapunov function

$$L = k_Q[(1 - k_\mu\mu_e)^2 + \boldsymbol{q}_e^T\boldsymbol{q}_e] = 2k_Q(1 - k_\mu\mu_e) \tag{32}$$

where $k_Q > 0$, $k_\mu = 1$ when $\mu_e \geq 0$ and $k_\mu = -1$ when $\mu_e < 0$. From (29), $\dot{L} = k_Qk_\mu\boldsymbol{q}_e^T\boldsymbol{\omega}_e$. Define $\bar{\boldsymbol{\omega}}_e = [\bar{\omega}_{ex}, \bar{\omega}_{ey}, \bar{\omega}_{ez}]^T = \boldsymbol{\omega}_e + k_\omega k_\mu\boldsymbol{q}_e$, where $k_\omega > 0$. Choose a Lyapunov function

$$L_1 = L + \frac{1}{2}\bar{\boldsymbol{\omega}}_e^T J\bar{\boldsymbol{\omega}}_e \tag{33}$$

$$\begin{aligned}\dot{L}_1 = \bar{\boldsymbol{\omega}}_e^T[&-\boldsymbol{\omega} \times J\boldsymbol{\omega} + \boldsymbol{\tau}_1 + J(S(\boldsymbol{\omega}_e)R^T(Q_e)\boldsymbol{\omega}_c - R^T(Q_e)\dot{\boldsymbol{\omega}}_c \\ &+ k_\omega k_\mu\dot{\boldsymbol{q}}_e) + \boldsymbol{\Delta}_\tau] - k_Qk_\omega\boldsymbol{q}_e^T\boldsymbol{q}_e + k_Qk_\mu\boldsymbol{q}_e^T\bar{\boldsymbol{\omega}}_e\end{aligned} \tag{34}$$

Design the control torque

$$\begin{aligned}\boldsymbol{\tau}_1 = &-k_\tau\bar{\boldsymbol{\omega}}_e + \boldsymbol{\omega} \times J\boldsymbol{\omega} - JS(\boldsymbol{\omega}_e)R^T(Q_e)\boldsymbol{\omega}_c + JR^T(Q_e)\dot{\boldsymbol{\omega}}_c \\ &- k_\omega k_\mu J\dot{\boldsymbol{q}}_e - \mathrm{Tanh}(\frac{\bar{\boldsymbol{\omega}}_e^T}{\varepsilon_4})\boldsymbol{\gamma} - k_Qk_\mu\boldsymbol{q}_e\end{aligned} \tag{35}$$

where $k_\tau > 0$ and ε_4 is a small positive constant. Substituting $\boldsymbol{\tau}_1$ into (34) yields

$$\dot{L}_1 = -k_Q k_\omega \boldsymbol{q}_e^T \boldsymbol{q}_e - k_\tau \bar{\boldsymbol{\omega}}_e^T \bar{\boldsymbol{\omega}}_e - \bar{\boldsymbol{\omega}}_e^T \mathrm{Tanh}(\frac{\bar{\boldsymbol{\omega}}_e^T}{\boldsymbol{\varepsilon}_4})\boldsymbol{\gamma} + \bar{\boldsymbol{\omega}}_e^T \boldsymbol{\Delta}_\tau \tag{36}$$

Theorem 2 *Take $k_\omega \le \frac{4k_\tau}{\bar{\lambda}(J)}$, the attitude controller (35) guarantees that the attitude tracking error $\boldsymbol{q}_e$ and angular velocity error $\boldsymbol{\omega}_e$ are bounded and ultimately converge to neighbourhoods of the origin.*

Proof From Lemma 2, $\bar{\boldsymbol{\omega}}_e^T \boldsymbol{\Delta}_\tau \le \sum_{i=x,y,z} |\bar{\omega}_{ei}|\gamma_i \le \sum_{i=x,y,z} [\bar{\omega}_{ei} \tanh(\frac{\bar{\omega}_{ei}}{\varepsilon_4}) + k_q \varepsilon_4]\gamma_i = \bar{\boldsymbol{\omega}}_e^T \mathrm{Tanh}(\frac{\bar{\boldsymbol{\omega}}_e}{\varepsilon_4})\boldsymbol{\gamma} + d_\tau$, where $d_\tau = \sum_{i=x,y,z} k_q \varepsilon_4 \gamma_i$. Substituting it into (36) yields

$$\dot{L}_1 \le -k_Q k_\omega \boldsymbol{q}_e^T \boldsymbol{q}_e - k_\tau \bar{\boldsymbol{\omega}}_e^T \bar{\boldsymbol{\omega}}_e + d_\tau \le -k_Q k_\omega (1 - k_\mu \mu_e) - \frac{k_\tau}{\bar{\lambda}(J)} \bar{\boldsymbol{\omega}}_e^T J \bar{\boldsymbol{\omega}}_e + d_\tau \tag{37}$$

From (33), $\dot{L}_1 \le -\min\{\frac{k_\omega}{2}, \frac{2k_\tau}{\bar{\lambda}(J)}\} L_1 + d_\tau = -\frac{k_\omega}{2} L_1 + d_\tau$. Integrating it gives

$$L_1 \le (L_1(0) - \frac{2d_\tau}{k_\omega}) e^{-\frac{k_\omega}{2}t} + \frac{2d_\tau}{k_\omega} \le L_1(0) e^{-\frac{k_\omega}{2}t} + \frac{2d_\tau}{k_\omega} \tag{38}$$

Also from (33) we know that $K_Q \boldsymbol{q}_e^T \boldsymbol{q}_e \le L_1$ and $\frac{\underline{\lambda}(J)}{2} \bar{\boldsymbol{\omega}}_e^T \bar{\boldsymbol{\omega}}_e \le L_1$. Thus $\boldsymbol{q}_e$ and $\bar{\boldsymbol{\omega}}_e$ are bounded and ultimately converge to the compact sets $\mathbb{C}_q = \{\boldsymbol{q}_e | \|\boldsymbol{q}_e\| \le \sqrt{\frac{2d_\tau}{k_Q k_\omega}}\}$ and $\bar{\mathbb{C}}_\omega = \{\bar{\boldsymbol{\omega}}_e | \|\bar{\boldsymbol{\omega}}_e\| \le \sqrt{\frac{4d_\tau}{\underline{\lambda}(J)k_\omega}}\}$. Since $\boldsymbol{\omega}_e = \bar{\boldsymbol{\omega}}_e - k_\omega k_\mu \boldsymbol{q}_e$, we have $\|\boldsymbol{\omega}_e\| \le \|\bar{\boldsymbol{\omega}}_e\| + k_\omega \|\boldsymbol{q}_e\|$, so $\boldsymbol{\omega}_e$ converges to the set $\mathbb{C}_\omega = \{\boldsymbol{\omega}_e | \|\boldsymbol{\omega}_e\| \le \sqrt{\frac{2k_\omega d_\tau}{k_Q}} + \sqrt{\frac{4d_\tau}{\underline{\lambda}(J)k_\omega}}\}$.

Remark 3 By taking $k_Q >> k_\omega$, increasing k_Q, k_w and decreasing ε_4, the sets $\mathbb{C}_q$ and $\mathbb{C}_\omega$ can be made small.

5 Simulation

A simulation is performed to verify the proposed controller. The helicopter parameters are as follows [12]: $m = 7.4\,\mathrm{kg}, I_x = 0.16\,\mathrm{kgm}^2, I_y = 0.30\,\mathrm{kgm}^2, I_z = 0.32\,\mathrm{kgm}^2, I_{xz} = 0.05\,\mathrm{kgm}^2, l_m = 0.01\,\mathrm{m}, h_m = 0.14\,\mathrm{m}, l_t = 0.95\,\mathrm{m}, h_t = 0.05\,\mathrm{m}, M_a = L_b = 110, A_m = 0.00452, B_m = 0.63, A_t = 0.005066, B_t = 0.008488$ and $g = 9.81\,\mathrm{m/s}^2$. The desired reference path $\mathcal{P}_r$ is a circular curve determined by

$$f_1(x, y, z) = z - 8 = 0, \;\; f_2(x, y, z) = \frac{1}{5}(x^2 + y^2) - 5 = 0$$

Define $P_0 = [11, 10, 0]^T$ and choose $P_d = [5, 0, 8]^T$, we can obtain the sphere center $\bar{O} = [11, 0, 0]^T$ and the temporary path $\bar{\mathcal{P}}_r$ is planned by

$$\bar{f}_1(x, y, z) = 4x + 3z - 44 = 0, \;\; \bar{f}_2(x, y, z) = \frac{1}{20}((x - 11)^2 + y^2 + z^2) - 5 = 0$$

where $\boldsymbol{\delta} = [1, 1, 1]^T$, $\boldsymbol{\gamma} = [0.5, 0.5, 0.5]^T$. The controller parameters are chosen as follows: $\bar{k}_{11} = \bar{k}_{12} = 1, \bar{k}_{21} = \bar{k}_{22} = 3.5, \bar{k}_{31} = 1, \bar{\varepsilon}_1 = 0.3, \bar{\varepsilon}_2 = 0.5, \bar{\varepsilon}_3 = 0.1; k_{11} = k_{12} = 2, k_{21} = k_{22} = 3.5, k_{31} = 3, \varepsilon_1 = 0.3, \varepsilon_2 = 0.8, \varepsilon_3 = 0.08; k_Q = 500, k_\omega = k_\tau = 16, \varepsilon_4 = 0.05; \xi = 0.707, \omega_n = 10, \bar{\varepsilon} = 0.01$, and they satisfy the conditions in theorems. Choose $\bar{v}_r = v_r = 2.5\,\text{m/s}$.

Figure 3 shows the 3-D path following result. Figures 4, 5 and 6 illustrate the path following, attitude and angular velocity errors respectively, which are bounded and converge to neighborhoods of origin. Figure 7 shows that the speed converges to v_r. Figure 8 illustrate u_{cz}(or $\bar{u}_{cz}$ before switch) is greater than zero, implying that no singularity occurs in deriving command attitude.

Fig. 3 3-D path following

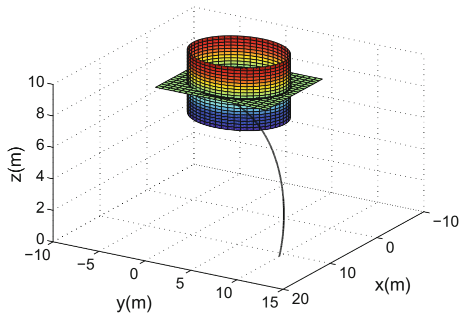

Fig. 4 Values of $\bar{\varsigma}_1, \bar{\varsigma}_2, \bar{\varsigma}_3, \varsigma_1, \varsigma_2, \varsigma_3$

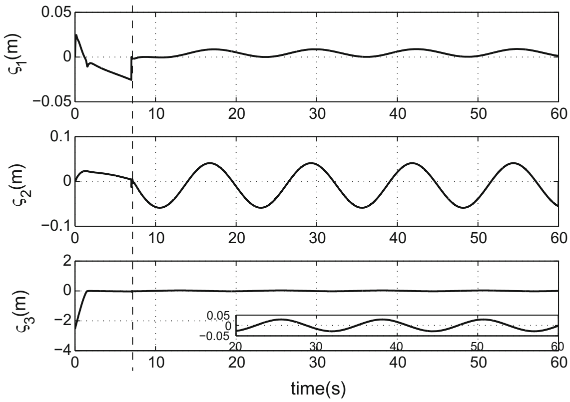

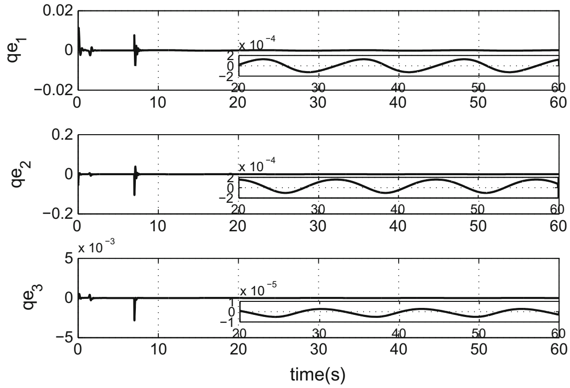

Fig. 5 Attitude tracking errors

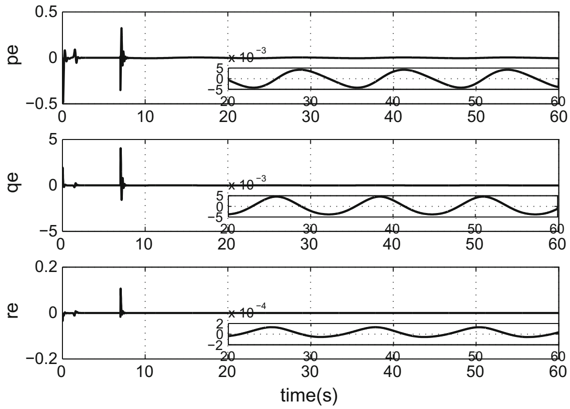

Fig. 6 Angular velocity tracking errors

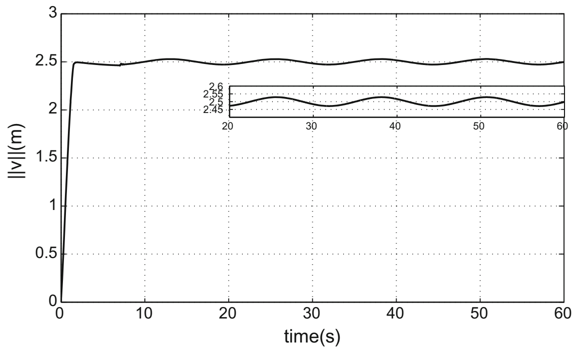

Fig. 7 Actual speed $\|\boldsymbol{v}\|$

Figures 9 and 10 show comparisons of spatial distance d_s, which defines the shortest distance from actual position to the path, and thrust T_m using the proposed control law and d_{s1}, T_{m1} using the control law [1] without temporary-path generation. Obviously, T_{m1} is large in convergence process, and it would result in control saturation if further increasing parameters to reduce the error.

Fig. 8 Control $\bar{u}_{cz}$ and u_{cz}

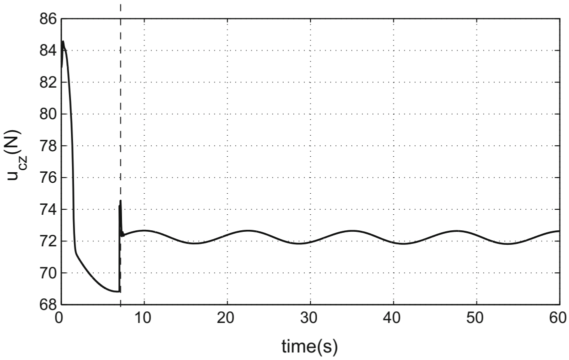

Fig. 9 Comparison of d_s and d_{s1}

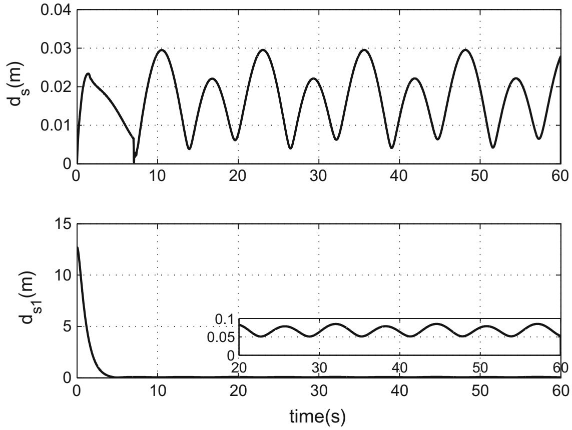

Fig. 10 Comparison of T_m and T_{m1}

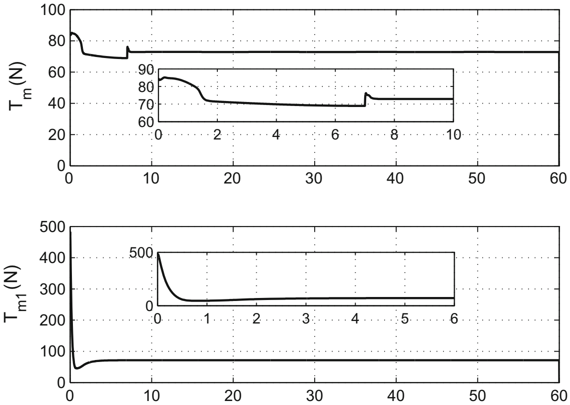

6 Conclusion

This paper presents a singularity-free path following controller for miniature unmanned helicopters. The reference path is defined by implicit expression. Numerical simulation demonstrates the effectiveness of proposed controller. In future research we will extend the controller to more general manifolds and consider the disturbances and parametric uncertainties.

Acknowledgements This work was supported by National Natural Science Foundation of China under Grant No. 61673043.

References

1. Zhu B, Huo W. 3-D path-following control for a model-scaled autonomous helicopter. IEEE Trans Control Syst Technol. 2014;22(5):1927–34.
2. Aguiar AP, et al. Performance limitations in reference tracking and path following for nonlinear systems. Automatica. 2008;44(3):598–610.
3. Huo W, Wang Q. Path following controller design for miniature unmanned helicopters. In: Control conference IEEE. 2011. p. 3537–3542.
4. Wang B, Dong X. Cascaded control of 3D path following for an unmanned helicopter. In: Cybernetics and intelligent systems IEEE. 2010. p. 70–75.
5. Wang T, et al. Combined of vector field and linear quadratic Gaussian for the path following of a small unmanned helicopter. Iet Control Theory Appl. 2012;6(6):2696–703.
6. Cabecinhas D, Cunha R, Silvestre C. A globally stabilizing path following controller for rotorcraft with wind disturbance rejection. IEEE Trans Control Syst Technol. 2015;23(2):708–14.
7. Roza A, Maggiore M. Path following controller for a quadrotor helicopter. In: American control conference IEEE. 2012. p. 4655-4660.
8. Qiang W, Huo W. Adaptive path-following control for miniature autonomous helicopter. Acta Armamentarii. 2012;33(11):1364–72.
9. Gandolfo. Path following for unmanned helicopter: an approach on energy autonomy improvement. Inf Technol Control. 2016;45(11).
10. Hua, Duc M, et al. Introduction to feedback control of underactuated VTOLvehicles: a review of basic control design ideas and principles. IEEE Control Syst. 2013;33(1).
11. Raptis IA, Valavanis KP, Moreno WA. A novel nonlinear backstepping controller design for helicopters using the rotation matrix. IEEE Trans Control Syst Technol. 2011;19(2).
12. Zou Y. Trajectory tracking ocntrol developments for miniature unmanned helicopters. PhD Dissertation. Beihang University, Beijing, China. 2016.
13. Polycarpou MM, Ioannou PA. A robust adaptive nonlinear control design. Automatica. 1996;32(3):423–7.
14. Farrell, Jay A, et al. Command filtered backstepping. IEEE Trans Autom Control. 2009;54(6):1391–1395.
15. Tayebi A. Unit quaternion-based output feedback for attitude tracking problem. IEEE Trans. Autom. Control. 2008;53(6):1516–20.